Blue autofluorescence in protein aggregates *"lighted on"* by UV induced oxidation.

A.Fricano[1,2], F. Librizzi[3], E. Rao[4^], C. Alfano[2] and V. Vetri[4]*

[1.] Dipartimento Biomedico di *Medicina* Interna e Specialistica, Università di Palermo, Piazza delle Cliniche 2 90127 Palermo

[2.] Fondazione Ri.Med, Via Bandiera, 11, 90133 Palermo

[3.] Institute of Biophysics, UOS Palermo, National Research Council, Via Ugo La Malfa 153, 90146 Palermo

[4.] Dipartimento di Fisica e Chimica, Università di Palermo, viale delle Scienze ed. 18, 90128 Palermo.

***corresponding author** To whom correspondence should be addressed.

^current address: Institute of Biophysics, National Research Council, Palermo, Italy.

Keywords

Ubiquitin, oxidative stress, amyloid autofluorescence, dityrosine formation, Fluorescence lifetime imaging.

A.

Abstract

Oxidation of amino acid side chains in protein structure can be induced by UV irradiation leading to critical changes in molecular structure possibly modifying protein stability and bioactivity.

Here we show, by using a combination of multiple spectroscopic techniques and Fluorescence Lifetime Imaging, that UV-light exposure induces irreversible oxidation processes in Ubiquitin structure. In particular, the growth of a new autofluorescence peak in the blue region is detected, that we attribute to tyrosine oxidation products. Blue autofluorescence intensity is found to progressively increase also during aggregation processes leading to the formation of aggregates of non-amyloid nature.

Significantly, analogous spectral modifications are found in amyloids fibrils from human insulin and Amyloid-β peptide grown under UV exposure. Experimental results reveal a substantial overlap between the fluorescence signal here attributed to tyrosine oxidation and the one referred in literature as "Amyloid autofluorescence". These findings clearly represent a caveat about the specificity of the blue fluorescence peak measured for amyloids, especially when grown in conditions in which tyrosine residues may be oxidized.

Moreover, our results once again highlight the close link between the formation of amyloid aggregates and protein damages resulting from oxidative stress, as these neurotoxic aggregate species are found to contain damaged residues.

Introduction

During their biological lifetime, proteins are frequently subjected to oxidation processes which may result in native structure damages, from backbone cleavage or protein crosslinking to subtler modifications such as side chain oxidations[1]. These modifications are involved in many aspects of cellular functions and result in the diversification of protein conformation, stability and protein-protein interactions [1,2]. Oxidation processes have been related to aging and to other pathologies being involved as a pathogenic mechanisms in neurodegenerative disorders like Alzheimer's and Parkinson's disease[2] and in many chronic diseases such as cancer, arthritis, cardiovascular diseases, diabetes[3,4] .On the other hand, these modifications have also found to be implicated in regular function of cells as for example in cell signaling[5,6].

Protein oxidation is known to be promoted by several factors: reactive oxygen species (ROS); ionizing radiations (X-rays, γ-rays, ultraviolet-light); activation of neutrophils and macrophages; oxidase-catalyzed reactions; lipid peroxidation and glycation/glycoxidation reactions[7,8,9].

Among effectors inducing oxidation, ultraviolet (UV) light deserves special consideration as most living systems are continuously exposed to sun-light. The solar UV radiation spectrum (wavelengths 100–400 nm) includes UVC (<280 nm), UVB (280–320 nm) and UVA (320–400 nm). Interestingly, it was shown that UVA radiation may interact with photosensitive molecules in cellular environment e.g. DNA, lipids and proteins and it is also responsible for generating ROS species[10]. The interest on the effects of UV-induced oxidation on the structure and function of proteins has increased in recent years, both for its pharmaceutical implications, as many protein-based drugs were found to be damaged from light, and for its medical consequences, as for example the exposure to UV component of solar radiation may cause physiological damages to skin. Direct photo-oxidation arising from the absorption of light by protein chromophores or complex phenomena mediated by UV- light may occur[11] which have to be elucidated together with

their consequences. Knowledge on molecular mechanisms involved in tissues responses to UV irradiation may provide useful insights on understanding skin-aging and provide new tools to develop therapeutic strategies against it.

Photochemical reactions induced by UV irradiation on proteins have as main target the aromatic (tryptophan, tyrosine, phenylalanine) and cysteine residues[12]. UV irradiation may induce tryptophan oxidation to form N-formylkynurenine, tyrosine oxidation to form 3,4-dihydroxyphenylalanine (DOPA), oxidation of leucine resulting in the formation of various hydroxyleucines, histidine oxidation to form aspartate or asparagine, and methionine oxidation to form methionine sulfoxide[13]. These residues can be modified in different rates and in dependence on protein structure and this may lead to changes in secondary and tertiary structure of proteins, in their stability, bioactivity, and immunogenicity[1,2,12,13].

Oxidation reactions can also mediate both intramolecular and intermolecular cross-linking of peptides and proteins, as it is in the case of dityrosine formation, which has been proposed as an important marker of oxidative stress [14,15,16]. Dityrosine is formed by covalent photochemical linkage between two proximal tyrosine residues; its formation leads to the appearance of a characteristic fluorescence band, not observed in standard tyrosine samples, with excitation/emission maxima at around 320/400 nm[16,17]. Moreover, the oxidation of tyrosine to DOPA, leads to the appearance of another peak in UV region with excitation/emission maxima at around 370/450 nm [18,19]. Functional consequences of these modification have been observed and interestingly the formation of dityrosine was suggested to play an important role in assembly and toxicity of α-synuclein in PD[20].

Recent studies on Human Insulin samples have shown that UV light irradiation induces significant changes in protein conformation which affects the hormone's structure and bioactivity[21]. Observed damages include tyrosine oxidation, insulin dimerization, disulphide bond disruption, secondary

and tertiary structure changes, and loss of biological function[21]. Interestingly, it was found that UV-light readily induces dityrosine formation in α-synuclein strongly affecting its amyloid formation mechanisms[22].

We report here an experimental study focused on the effects induced by UV radiation on proteins, in particular focusing on the UV- induced reactions in Ubiquitin (UBQ). We observed changes induced by UV stress on UBQ during its aggregation process highlighting light induced modifications.

UBQ is a small protein that plays a central role in intracellular proteolysis in eukaryotes[23]. It consists of a single polypeptide chain of 76 amino acid residues. This protein is ubiquitous in eukaryotes and highly conserved among species[23]. UBQ has been widely used as a model protein in the field of protein chemistry, for its unique physicochemical and biological properties. Importantly, for this study, its sequence is characterized by the presence of a unique Tyr residue, and by the absence of tryptophans and of disulphide bonds thus constituting a perfect system to single out, among the different processes brought about by UV irradiation on proteins, the oxidative effects on tyrosines[24,25].

UBQ targets damaged proteins destined for degradation through the multi-enzymatic complex of the proteasome, the dysfunction of degradation mechanisms has been reported in the pathogenesis of some diseases, certain malignancies, neurodegenerative disorders, and pathologies of the inflammatory immune response[26,27]. Interestingly, a relation between structural and stability modifications[28,29] due to oxidative damages was suggested to be involved in these disorders even if a clear picture has not been reached yet.

In this experimental study, we achieved UV irradiation of UBQ sample in solution by using the Xenon lamp of a spectrofluorometer during kinetic measurements. This allows to select specific

wavelength, to control exposure time and to simultaneously monitor the occurring changes. Modifications were observed in conditions promoting the aggregation of the protein.

In the presented conditions UV-irradiation leads to a change in the fluorescence signal, in particular the formation of a new band in the range 350-550 nm was observed, consistently with data reported in literature for the oxidation products of tyrosine residues[21,22].

Interestingly, we observed analogous oxidative effects following UV exposure for other proteins and peptides, such as human insulin, and Aβ (1-40) peptide, but not for Bovine Serum Albumin (BSA). UBQ, insulin and Aβ peptide sizably differ in structure and conformation, but they are all characterized by the absence in their sequence of Tryptophan residues, which, as known, absorb UV light in the same region of tyrosines and are able to quench tyrosine fluorescence. Therefore, the similarity of the effects observed for these different proteins and their absence in BSA, which has two tryptophans, strongly indicate a specific role of Tyrosine residues in the observed phenomenon. Moreover, the spectral features of the newly "lighted on" blue autofluorescence in UBQ amorphous aggregates formed and in amyloid aggregates from insulin and Aβ (1-40) peptide, substantially overlap (both in terms of spectral range and lifetime distribution) with the one that was recently attributed to intrinsic fluorescence of amyloid structures[30].

Results and discussion

In this study we report spectroscopic analysis of modification of UBQ under UV exposure induced by excitation light from a standard fluorimeter during kinetic measurements.

In figure 1 a) the time evolution of fluorescence emission spectra of 0.5 mg/ml UBQ incubated at 60°C, for 24 hours, is reported. Spectra were acquired every 20 minutes with continuous excitation at 275 nm. Figure 1b) reports UBQ fluorescence emission spectra measured at room temperature before and after 24 hours. This highlights critical changes in fluorescence spectrum profile. The observed changes are irreversible and do not occur if the sample is not subjected to continuous UV irradiation. Figure 1 c) shows UBQ absorption spectra before and after incubation at 60°C for 24 hours, under continuous UV exposure induced by excitation light at 275 nm during the kinetic measurements in fig.1a) together (panel d) with the difference spectrum between treated and untreated sample which better highlights the occurrence of two new absorption peaks. CD spectra in the far UV region of the freshly prepared and of the treated samples are reported in panel e) show minimal changes at the secondary structure level induced by the described treatment.

As can be seen in fig. 1 a) decrease in fluorescence emission intensity at around 350 nm and an increase at around 450 nm occur, as indicated by arrows. The main peak at lower wavelength is attributable to the emission of the unique tyrosine residue of the protein[31,32,33]. This residue[34] in position 59 plays an important role in UBQ function and is the main responsible of intrinsic fluorescence of UBQ due to the lack of tryptophans in the protein sequence. The steady state fluorescence signal of tyrosine is known to be poorly sensitive to the polarity of environment[35] although it has been used in some instances to monitor protein conformational changes during unfolding and aggregation[32,36]. In the case of UBQ, time resolved fluorescence studies in the ps range have suggested that changes in Tyr quantum yield, which occur by varying pH, are due to

the interaction with other residues in the surroundings and to the formation tyrosine-carboxylate hydrogen-bonded complex and tyrosinate[31,37].

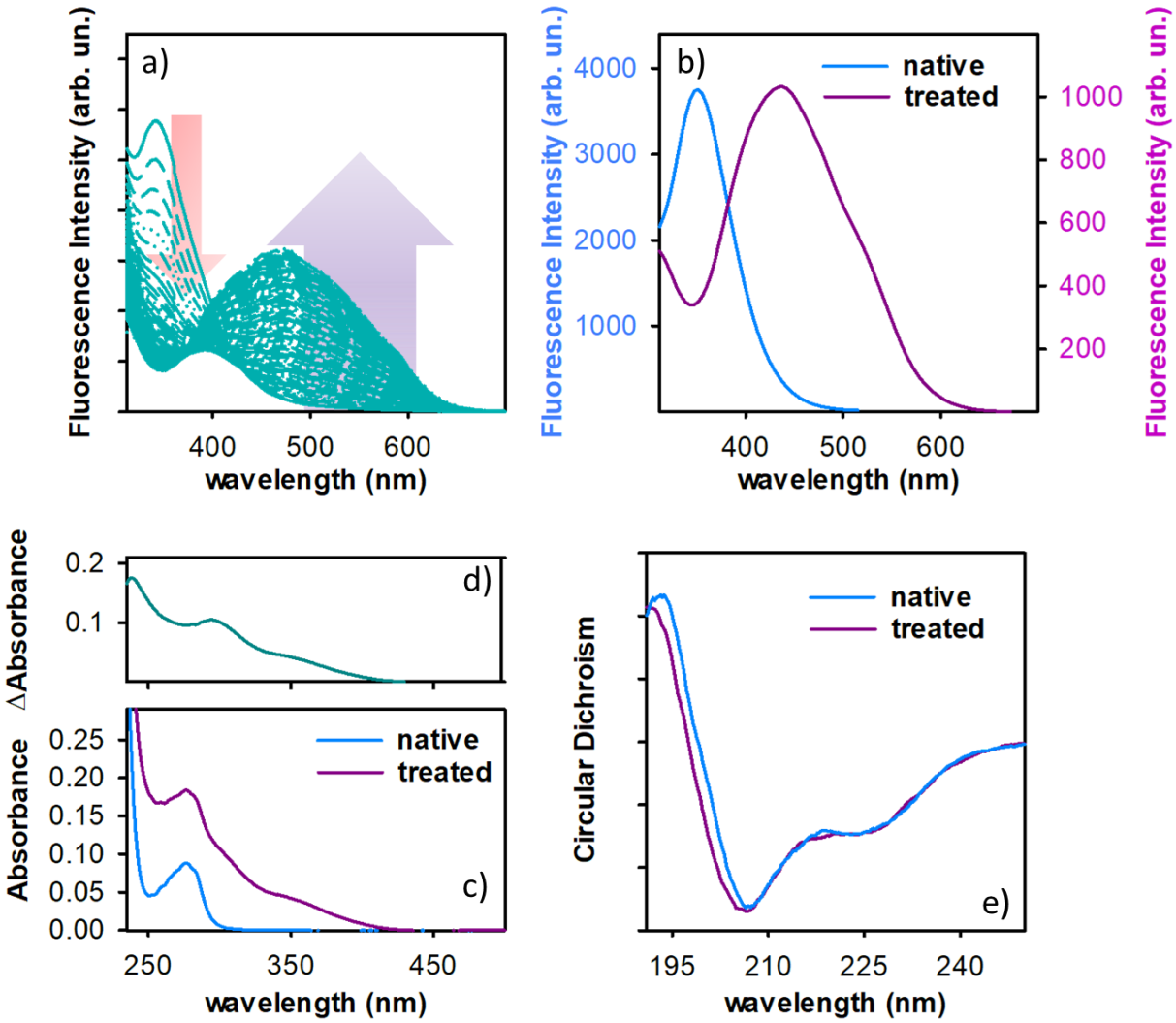

Figure1: (**a**) Time evolution of fluorescence emission spectra of 0.5 mg/ml UBQ in 20mM sodium phosphate buffer, pH 6.5, incubated at 60°C for 24h. Fluorescence spectra were acquired every 20 minutes with continuous excitation at λ_{exc}=275 nm. The arrows indicate the changes of the signals as a function of time. (**b**) Fluorescence emission spectra measured at room temperature of 0.5 mg/mL UBQ in 20mM sodium phosphate buffer, pH 6.5, before (blue line, blue axis) and after (purple line, purple axis) incubation at 60°C for 24h under continuous UV exposure. UBQ absorption spectra before and after thermal treatment at 60°C under UV exposure. **c**) Absorption Spectra of 0.5 mg/ml UBQ sample before (blue line) and after (purple line) incubation at 60°C for 24h, under continuous UV-exposure at UV-light at excitation wavelength at λ_{exc}=275 nm. **d**) Differential Absorption spectrum due to the continuous UV exposure. e) Circular Dichroism spectra of 0.5 mg/mL UBQ sample before (blue line) and after (purple line) treatment.

Measurements represented in figure 1a) reveal a progressive reduction of fluorescence intensity of tyrosine signal which occurs almost in parallel with the growth of a new peak centered at about 470 nm. Data do not show the presence of an isosbestic point thus indicating that the observed changes are not due to a simple conversion between two species. Multiple phenomena probably concur in the modification of the optical properties of the sample. Most likely, the observed spectral changes arise from the formation of tyrosine oxidation products [17], involving cyclization, decarboxylation and so on [38]. The oxidation of tyrosine residues results in the formation of different products, which are known to have optical activity [39], such as dityrosine [33,40] , Dihydroxyphenylalanine (DOPA) and some hydroxycinnamoyls [19]. Dityrosine formation upon UV irradiation, in particular, is widely discussed in the literature, associated with spectral changes similar to those reported in figure 1[21,41]. As an example, in the case of alpha-synuclein the growth of a fluorescence signal in this region occurring in parallel with the decrease of tyrosine fluorescence peak in the UV region was attributed to the formation of dityrosine [22] and specifically also to UV induced formation of di-tyrosine[20].

Modifications in absorption spectrum of the treated sample are evident as shown in fig 1c): incubation at 60 degrees brings about an overall increase of turbidity, attributable to an increased scattering of the solution, due to aggregation [42]. Most interestingly, following irradiation, changes are observed also in the absorption spectrum. In fact, as better shown in panel d), UV exposure leads to the growth of two new significant components, one centered at about 300 nm and one, more evident, centered at 350 nm. These findings are in line with the formation of tyrosine oxidation products. In particular, similar modifications in the absorption spectrum are considered, together with the appearance of a fluorescence peak in the blue range as the one reported in fig. 1 a) and b), as a marker of di-tyrosine formation, which have been associated to aging processes or exposure to UV-light[43]. Notably, analogous measurements performed in the same conditions on

Bovine Serum Albumin, whose structure presents 2 tryptophan residues, do not lead to the growth of new fluorescence or absorbance peaks, like those shown in Figs. 1 a-d). The lack of these phenomena in the presence of tryptophan residues, which absorb light in the same region clearly confirms the specific role, in the case of UBQ, of its single tyrosine residue. Moreover, SDS PAGE on an analogous UBQ sample before and after the treatment confirms that aggregation occurs (data not shown).

To confirm the role of UV-irradiation in the observed spectral changes, we performed a series of experiments with different degrees of UV-exposure.

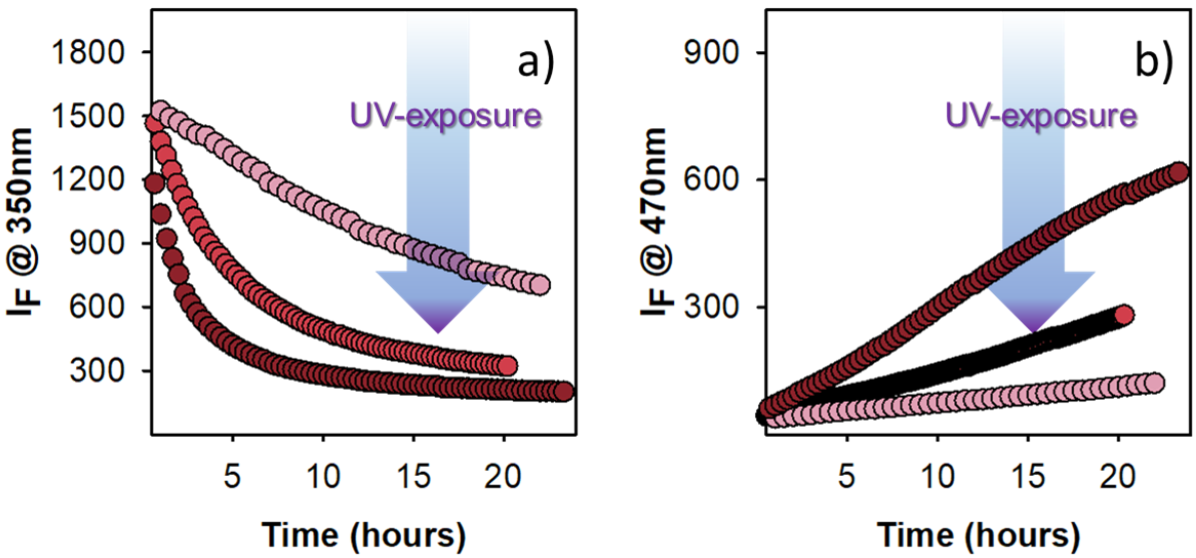

Figure 2: Fluorescence emission intensity as a function of time measured at 350 nm **a**) and at 470 nm **b**) for 0.5 mg/ml UBQ in 20mM sodium phosphate, pH 6.5, incubated at 60°C for 22 hours; Ubiquitin was exposed to UV light (λ_{exc}=275 nm), continues UV-exposure (dark red circles), for 3 minutes (time of spectrum measurement) every 6 minutes (red circles), and for 2 minutes every 30 minutes (pink circles)

We report in Fig. 2 the kinetics of fluorescence spectral changes for three identical UBQ samples, incubated in the same conditions as before, but subjected to three different protocols of

excitation/irradiation during the fluorescence measurements: continuous excitation (dark red circles), excitation only for the duration of spectrum acquisition every 6 minutes (red circles) and every 30 minutes (pink circles). The time evolution of fluorescence intensity measured at 350 nm and at 470 nm are reported in figure 2a) and 2b) respectively. The reported data clearly show that the effects observed on UBQ fluorescence properties strongly depend on the extent of UV-exposure, being faster and more pronounced at increasing irradiation levels. Interestingly, the growth of signal at 470 nm (Fig. 2b) keeps going at longer times with respect to the decay of the tyrosine intrinsic fluorescence peak (Fig. 2a).

We recall again that in our experimental conditions the effects of UV-irradiation on UBQ spectral properties shown in Figs. 1 and 2 are entangled with protein supramolecular assembly which may favor tyrosine's exposure and modification. We report in the following measurements aimed at clarifying whether or not intermolecular interaction and supramolecular assembly are critically involved in tyrosine oxidation.

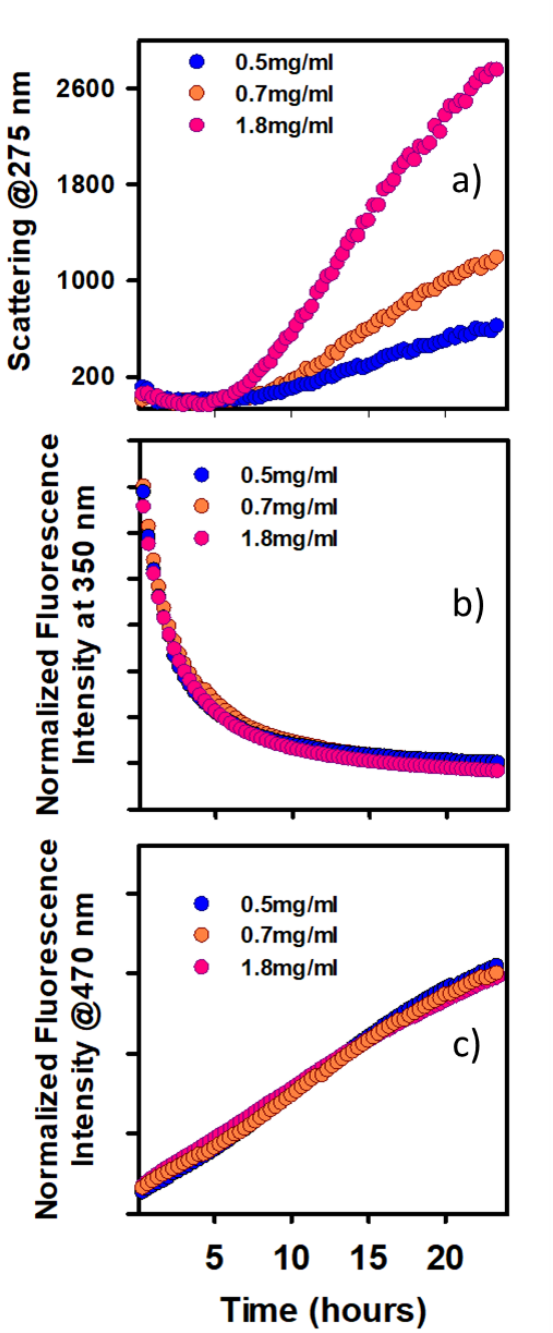

Figure 3: **a)** Rayleigh scattering intensity measured at 275 nm (corresponding to the excitation light in fluorescence measurements) as function of time, for three different UBQ concentrations. Measurements are acquired in the same experimental conditions as in fig 1 during kinetic fluorescence measurements under continuous illumination by excitation light. **b)** and **c)** Normalized fluorescence emission intensity as a function of time measured respectively at 350 nm (b) and at 470 nm (c), at different protein concentrations.

UBQ samples at three different protein concentrations were incubated at 60°C, under continuous exposure to UV-light for 24 hours during kinetic fluorescence measurements.

Fig. 3 shows the time evolution of Rayleigh scattering (a) and of fluorescence intensity measured at 350 nm (b) and at 470 nm (c) respectively. For the sake of comparison, fluorescence signals have been normalized to the first measurement intensity value. Fig. 3a) shows that after a lag-phase lasting about 5 hours, the Rayleigh scattering intensity starts to increase as function of time. The observed growth depends on protein concentration and leads to larger intensity values at higher concentrations and it is certainly related to aggregates growth in solution[42]. The detailed analysis of UBQ aggregation mechanisms in these conditions is clearly out of the scopes of this study. We report data in fig. 4a) to note, that while Rayleigh scattering (fig. 4a), here used as a measure of aggregation in solution, starts to increase only after few hours of incubation, fluorescence spectral changes are observed since the very beginning of the kinetics (Fig. 4b, c), strongly suggesting a disentanglement between the two processes.

To further confirm this statement, we performed analogous experiments in conditions in which no massive supramolecular aggregation is observed.

Figure 4 shows a comparison between data obtained at high temperature (60°C, as for the experiment up to now discussed) and at 25°C. Rayleigh scattering indicates that no aggregation occurs at 25°C (Fig. 4a), while spectral modifications can still be observed (Fig. 4b), even if with a lower rate than at 60°C.

It is not possible to directly compare the absolute fluorescence values because of the intrinsic dependence of fluorescence signal on temperature; however, in both conditions significant changes are observed whose rate depends on temperature. In figure 4 c) the variations of fluorescence emission intensity at 470 nm are reported, dashed grey lines are used as eye guide to highlight the different slopes of the two kinetics and to elicit the change of slope occurring at higher temperature which is not observed in the sample at 25°C within the experimental observation time. Measures in fig. 4 highlight that the effect of temperature and UV-light cannot

be easily disentangled but the variation of signal attributed to the formation of tyrosine oxidation products occurs both at 60°C i.e. in conditions were aggregation occurs and at 25°C i.e. in conditions were aggregation is not observed. Quite plausibly, high temperature facilitates the oxidative processes induced in tyrosine by UV-irradiation.

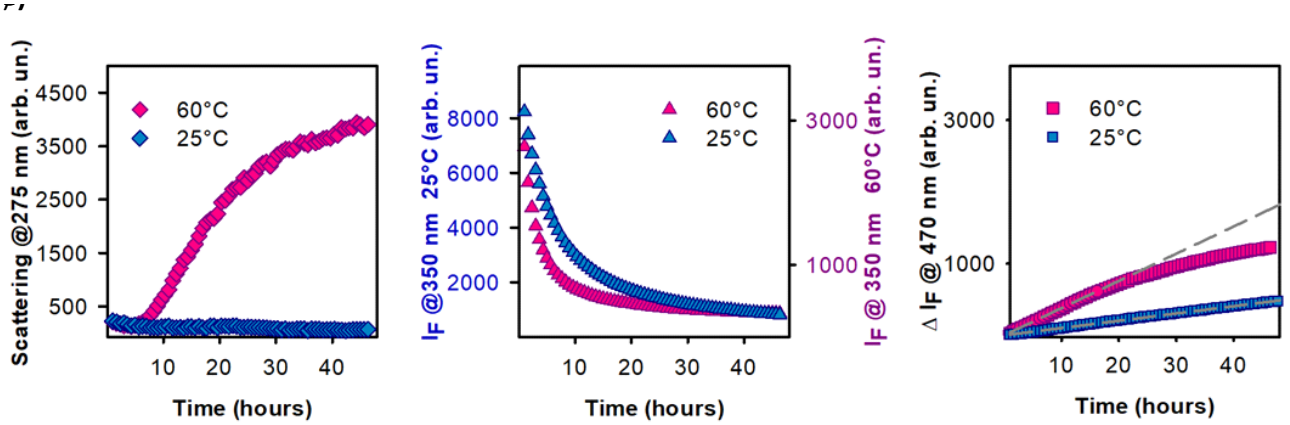

Figure 4: Rayleigh scattering intensity at 275 nm (corresponding to the excitation light in fluorescence measurements) as function of time **a**). Fluorescence emission intensity as a function of time, measured at 350 nm **b**) at 470 nm **c**) for UBQ at a concentration of 1.8 mg/ml UBQ, incubated at 60°C and at 25°C. In panel c, dashed grey lines are guide to the eye, to highlight the different rates in the increase of the fluorescence intensity measured at 470 nm. Measurements are acquired during kinetic fluorescence measurements under continuous illumination by excitation light.

Furthermore, UBQ aggregation can be induced also at low temperature by subjecting the sample to stirring (see Fig. 5a). The comparison between the fluorescence data observed with or without stirring (Fig. 5 b and c) again confirms that the concomitance of aggregation has no effect at all on the kinetics of the spectral changes occurring in tyrosine fluorescence. For the sample under stirring the monotonic decrease of fluorescence intensity at 350 nm is observed from the initial

stage during the lag phase of aggregation. Fluorescent spectra modifications overlap, within the experimental error, both in stirring and quiescent conditions.

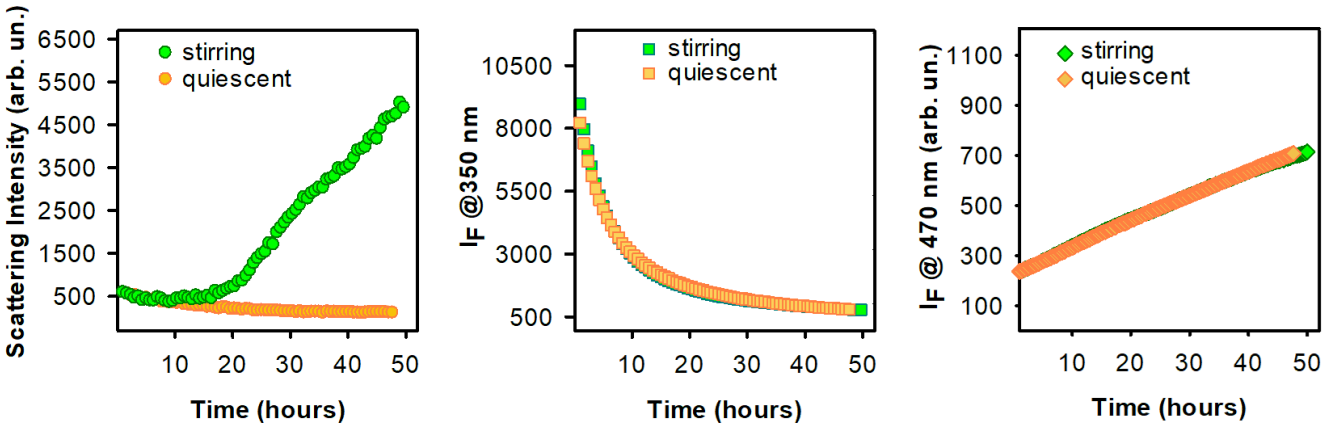

Figure 5: Rayleigh scattering intensity at 275 nm (i..e corresponding to the excitation light in fluorescence measurements) **a)** and Fluorescence emission intensity measured at 350 nm **b)**, and at 470 nm **c)** as a function of time. 1.8 mg/ml UBQ samples in 20mM sodium phosphate, pH 6.5, for 48h were incubated at 25°C, stirring at 500 rpm (green symbols) and in quiescent conditions (orange symbol). Measurements are acquired during kinetic fluorescence measurements under continuous illumination by excitation light.

In sum, all data reported indicate that UV exposure induce modifications in UBQ UV-Visible absorption and in its fluorescence signal that can be ascribed to the formation of tyrosine oxidation products. This process is facilitated by high temperature (Fig. 4) but occurs both in aggregation conditions and in conditions were massive supramolecular association is not observed (Figs. 4 and 5).

The spectral changes induced in tyrosine fluorescence by UV-exposure are reported in details in Fig. 6a), which reports in a contour plot the fluorescence emission intensity in the 350-700 nm region as a function of excitation wavelength light in the range 280- 450 nm for an analogous UBQ sample, after incubation at 60°C for 72 hours under continuous UV light exposure. Different

emission profiles for selected excitation wavelengths are shown in Fig. 6b), while the differential absorption spectrum is reported as a reference in fig. 6c).

Fig. 6 shows that the fluorescence emission peak can be excited not only at wavelengths typically attributed to tyrosine residues (<290nm), but at higher wavelengths, which correspond to the new absorption bands observed after treatment and allow to isolate the newly formed fluorescence band from the typical tyrosine fluorescence peak. Specifically, we note that the fluorescence signal in the blue range (i.e. above ~450 nm) can be detected also at excitation wavelengths above 350 nm.

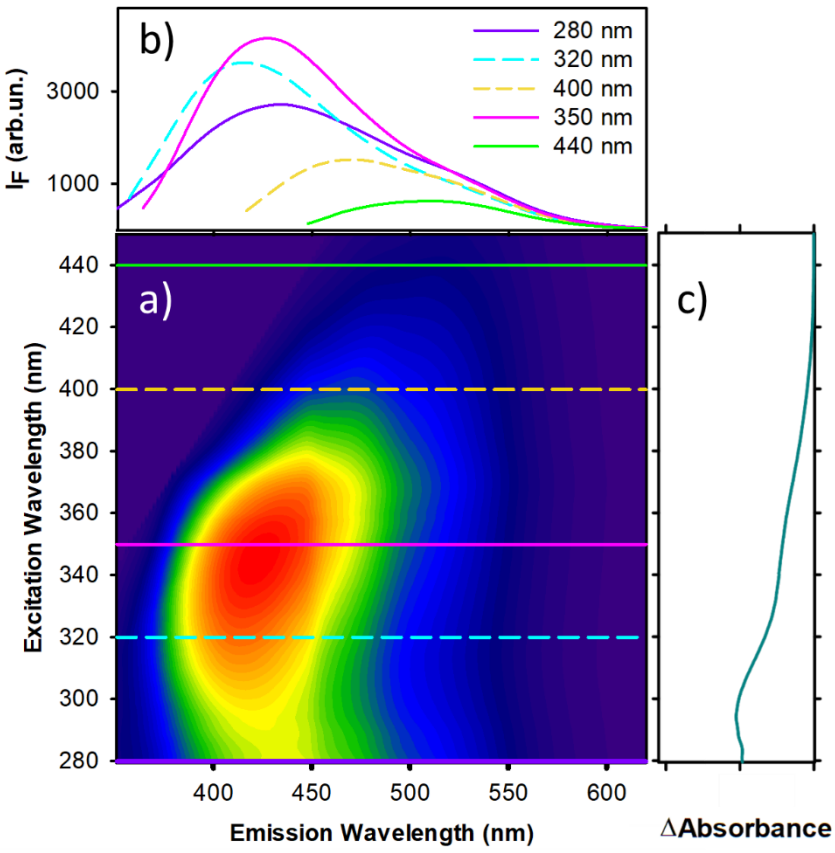

Figure 6: 3D fluorescence spectra/contour maps acquired at room temperature for UBQ (1.8 mg/ml) sample, after incubation at 60°C for 72 hours, under continuous excitation at 275 nm. **a)** Horizontal lines indicate the excitation wavelengths relative to representative emission spectra, which are reported in panel **b**. **c)** Differential adsorption spectrum between treated and native sample, showing the variations in absorption profile due to the treatment.

3D-fluorescence spectra reported in Fig. 6a) reveal the complex nature of the newly formed species.

It can be inferred that the fluorescence signal of the treated sample arises from at least two energetic levels which correspond to different species, induced by UV-exposure. These changes can be attributed to the formation of tyrosine oxidation products such as Tyrosinate (emission maximum at 430 nm) and di-tyrosine (maximum peak at 410nm) , which can be formed under our experimental conditions[16,17,19].

We believe important to note that all the UBQ samples analyzed in this work, where aggregation occurred, were found to be negative to Thioflavin T (ThT) test. As very well known, this dye is widely used to specifically detect and characterize amyloid fibrils[44,45] and, with some precautions [46,47] its fluorescence signal can be used as a good indicator of the amount of fibrillar aggregates in the sample. The absence of ThT fluorescence exclude the amyloid nature of the aggregates formed in our samples, as also confirmed by Circular Dichroism in fig. 1 d) and FTIR measurements on the sample obtained at higher concentration with longer exposure (reported in supplementary materials fig. S1), in which no evidence was observed for a transitions to beta-sheet structure typical of amyloid fibrils. The above observations rule out any possible contribution in all the above reported measurements of the so called Amyloid autofluorescence[48].

Interesting results on the properties of the new fluorescence bands induced by UV-exposure in UBQ can be obtained by Fluorescence Lifetime Imaging, also in comparison with analogous measurements performed on Insulin and Amyloid β samples, which, under suitable conditions, easily forms amyloid fibrils.

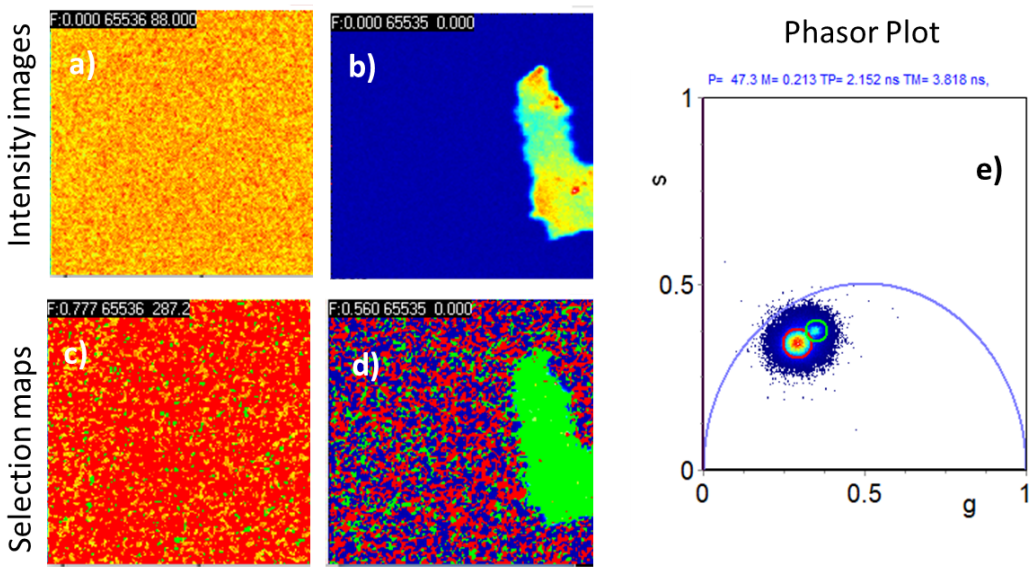

Figure 7: Fluorescence intensity images (60µm x 60µm) of 1.8 mg/ml UBQ after incubation at 60°C for 72 h, under continuous UV-exposure during fluorescence measurements using at λ_{exc}=275 nm. Panel **a)** shows a region of the sample with species under resolution and panel **b)** an area with large aggregates. **c)** and **d)** Selection maps of UBQ, corresponding to the fluorescence images a) and b), respectively. Pixel are colored depending on their lifetime values. **e)** Phasor plot, showing the distribution of UBQ lifetimes after treatment. Red and green cursors select two different lifetime distributions. The size of the images is 60 µm (a and b). Excitation wavelength for two photon imaging was λ_{exc}: 780nm; Detection range: 430-700 nm.

In figure 7 fluorescence lifetime imaging microscopy (FLIM) measurements on aliquots of the 1.8 mg/ml UBQ after incubation at 60°C for 72 h are shown. We report representative intensity images of two region of the sample, one where a uniform distribution of fluorescence is measured attributable to the presence of species with size under instrumental spatial resolution (a) and one where, together with diffuse fluorescence signal, a micrometric size aggregate is present, characterized by higher intensity (b). Images are acquired under two photon excitation at 780 nm i.e. at an excitation wavelength corresponding to the larger intensity of the fluorescence emission band centered at 430 nm.

FLIM measurements were analyzed by means the so called phasor approach[49,50] and the corresponding maps (Fig. 7c),d)) and phasor plot (Fig. 7e)) are reported. The output of phasor analysis gives a graphical view of all the measured fluorescence decays at each pixel in the images. In the phasor plot each point represents the fluorescence lifetime at each image pixel. Single exponential lifetimes are represented as points laying on the so called "universal circle"[49]. Longer lifetimes are mapped near the origin and shorter lifetimes are mapped on the circumference toward the bottom right intersection with the x axis. Lifetime values are determined by the position of the phasor in the universal circle, after system calibration (see methods for details). The clouds of points representing the fluorescence lifetime distribution over the two images are selected using a colored cursor and the corresponding pixels are mapped back with the selected color to the image.

In phasor plot (figure 7e)) the distribution of fluorescence lifetimes values is reported. As can be seen, the measured lifetime distribution presents two almost overlapping components. Red and green cursors were used to select in the image pixels with corresponding lifetimes in the selection maps (figures 7c), d)). Interestingly, pixels selected by red cursor (where the faster component is dominant) are in regions were only sub-resolution species are located and where lower intensity is measured. On the contrary, pixels selected by the green cursor (slower component) are on bright macroscopic aggregates. The complexity of the measured lifetime distribution may obviously arise from the micro environmental properties of the fluorophore surroundings. The properties of the fluorescence signal from the same chromophore(s) may change due to different environment experienced in small structures or in large aggregates and/or may originate from different tyrosine oxidation products.

We performed analogous experiments also on insulin and Aβ(1-40) peptide, following prolonged UV exposure during aggregation process. Insulin and Aβ(1-40) peptide were selected for their

ability to form amyloid fibrils and for the lack in their sequence of tryptophan residues. An additional element of interest can arise from the evidences reported in literature, indicating that oxidative stress can be a deleterious factor in neurodegenerative diseases such as Alzheimer's and Parkinson's disease[51], and could also induce insulin resistance involved in Type II diabetes[52], being a link between these pathologies[53,54]. Further, the formation of dityrosine and DOPA has been widely reported in a number of diseases[2,22,55].

Both insulin and Aβ easily undergo the same spectral modifications above reported for UBQ, following incubation under UV light excitation at 275 nm (see Supplementary materials fig S2 and S3) FLIM measurements (Fig. 8) clearly show the presence of newly formed fluorescent species whit analogous properties as the ones reported in fig. 7. Fig. 8 in particular shows a comparison between FLIM measurements on UBQ, Insulin and Aβ(1-40) aggregates. No fluorescence signal is observed on native protein samples in these conditions. We recall again that both Aβ and insulin are able to easily form amyloid fibrils. Actually, we incubated these proteins in conditions favoring their amyloid aggregation, in both cases, clearly, always under continuous UV-exposure (λ_{exc}=275 nm). As a consequence, at difference from UBQ, these samples resulted strongly positive to ThT, confirming the formation of amyloid fibrils (Fig. S2 and S3).

Representative images of UBQ, Human Insulin and Aβ(1-40) samples are reported in fig. 8 a), b) and c) respectively. In panel g) the phasor plot relative to all the images is reported. The red cursor is used to select pixels with the same lifetime distribution, highlighted in red in panel e) for UBQ, f) for Insulin and g) for Aβ (1-40).

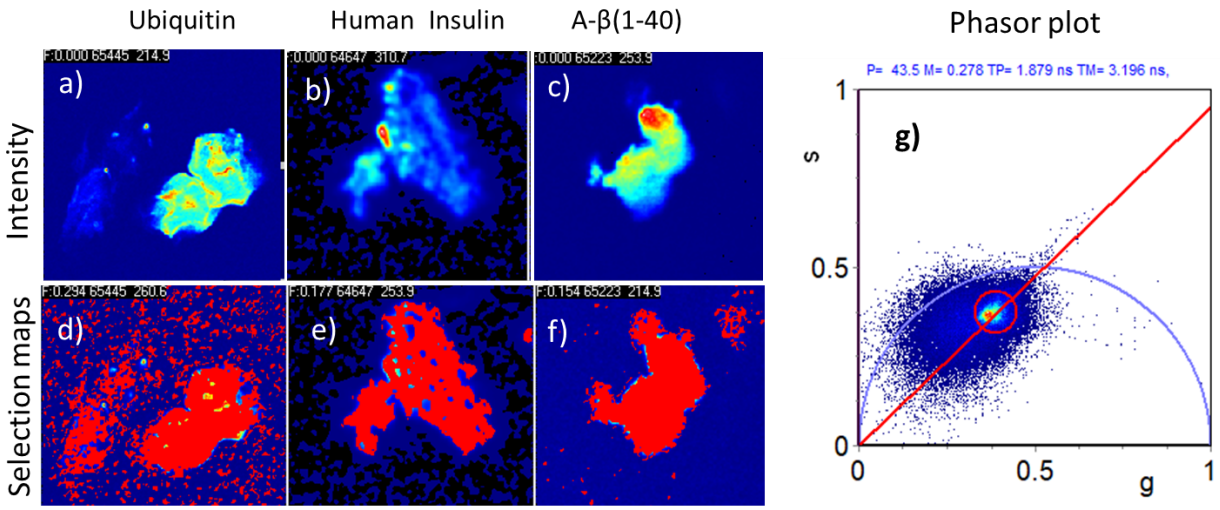

Figure 8: Fluorescence intensity images of UBQ **a)**, Human Insulin **b)** and Aβ(1-40) **c)**; **d)**, **e)** and **f)**: Selection maps corresponding to the same regions. **g)** Phasor plot representing the distribution of lifetimes in every pixel in the presented images. Red cursor is used to select pixels with the same lifetime. All proteins were incubated under continuous irradiation at λ_{exc}=275 nm. Two-photon excitation wavelength was λ_{exc}=780 nm; Detection range: 430-700 nm.

In the selection maps (fig. 8 d-f) red pixels corresponding to the same lifetime in the phasor plot (fig.10 d) are picked. Interestingly, all the presented aggregates reveal an analogous lifetime distribution, strongly suggesting the same origin for the blue autofluorescence signal observed in all samples.

A common structural property of the samples analyzed in this work is the lack of tryptophan residues in their sequence. In fact, the extinction coefficient of tryptophan residues is ε_{trp} 5540 M^{-1} cm^{-1}, higher than ε_{tyr} 1480 M^{-1} cm^{-1} for tyrosine residues, this may reduce the effect of incident light on tyrosines[56]. Moreover, as well known, tryptophans are able to quench tyrosine fluorescence by resonance transfer mechanisms. Quite reasonably, this process can protect tyrosine residues

against UV-irradiation induced oxidation, by limiting the time spent by the fluorophore in the excited state[57]. As a control, analogous experiments were performed on Bovine Serum albumin in sodium phosphate buffer, pH 6.5 at 60°C and no significant spectral modifications were observed.

For all three samples reported in Fig. 8, after prolonged UV exposure we observed, under two photon excitation at 780 nm, an intrinsic blue fluorescence in the region 430-700 nm with the same lifetime distribution. Specifically, this intrinsic fluorescence was detected with identical properties in UBQ amorphous aggregates, not positive to ThT, and Insulin and Aβ fibrils, resulted to be positive to ThT. We have also shown for UBQ sample that the observed spectral modifications are independent on the aggregation state of the sample. We attributed these changes to the formation of oxidation products of tyrosine and in particular to dityrosine and DOPA.

As previously reported, the occurrence of a blue fluorescence in the same region has been observed for dityrosine formation in α-synuclein samples[58], and in Aβ (1-42) fibrils grown under oxidative stress conditions[59] in vitro. Moreover, it has been reported that UV-light illumination is able to induce visible fluorescence in the blue range in Amyloid beta deposits from human brain[60]. In addition, amyloid aggregates fluorescence, referred to as “amyloid intrinsic fluorescence”, has been reported with excitation and emission profile in the same regions as the ones here reported, and with analogous lifetimes, between 2 and 3 ns. The fibrils investigated in these studies were grown in conditions where tyrosine modifications could occur. Therefore, it is possible to infer that, among other factors, also tyrosine oxidation phenomena may contribute to the origin of this signal. As a further control we report in fig. S4 measurements on polyaniline amyloid fibrils which do not present in our experimental conditions any fluorescence signal in the UV visible range using λ_{exc} = 275 nm and 350 nm.

This result is in line with recent findings from Shirshin and coworkers who have shown, that fluorescence signal in the deep blue region can be related to formation of oxidation products, by ultrahigh resolution mass spectroscopy experiments on amyloid forming Lysozime, Insulin samples and single amino acids. In the selected experimental conditions, these authors have highlighted the role of high temperature as oxidation effector[61]. Together with the data presented here, these findings challenge the simple attribution of "amyloid intrinsic autofluorescence" and point the finger at the need for attention to details of sample preparation and to control experiments especially with the development of extremely sensitive instrumentation and automated methods and when aromatic residues are present in the sample.

The above observation can be of great interest, also because such processes may constitute a link between oxidative stress and amyloid related pathology. It clearly claims for further investigations and control experiments.

Conclusions

In this work we presented experimental data illustrating how UV light exposure induces the irreversible oxidation of the single tyrosine residue in UBQ structure. We have used spectroscopic techniques to study the effects induced by exposure to UV, that could cause changes in the structure of the protein and affect its biological function. The obtained results show that UV exposure causes dramatic changes in the spectral properties of UBQ, giving rise to fluorescence products in the blue range. Modifications in different extent depend on UV exposure time and on temperature and are evident both in aggregation promoting conditions and in conditions where macroscopic aggregation is not observed.

We analyzed the spectral properties of the newly formed fluorescence peak which are assigned to tyrosines oxidation products. In particular, we infer that this signal, in our experimental conditions,

mostly arises from dityrosine and tyrosinate formed under UV exposure. These molecules can be used as a spectral markers of oxidative stress both in vitro and in vivo [14,17,19] and can be identified by simple fluorescence measurements. We highlight the possibility of using FLIM and "phasor approach" as an important analysis tool in multiple applications in biotechnologies. In this instance, it enables to locate fluorescent aggregates with specific lifetime distributions, and easily compare them.

Moreover, we also report UV-light induced oxidation of tyrosine residues in two amyloidogenic proteins: Aβ (1-40) peptide, whose role in Alzheimer's disease is widely accepted [46,59] and human insulin, which constitute a prototype for amyloid formation studies and has well known applications has drugs. UBQ, Human insulin and Aβ (1-40) aggregates were analyzed by means of FLIM under the same measurement conditions. In spite of the fact that the aggregates formed by these proteins are different (amorphous for UBQ and amyloidal for Aβ and insulin), their characteristic blue autofluorescence presents analogous spectral properties and lifetime distribution, as shown by the "phasor approach".

Moreover, we wish to note that these results were obtained in standard measurements conditions, by using a commercial fluorimeter. Although modifications of protein samples using standard instrumentation has been reported before, for example using light with wavelength 220 nm from a Circular Dichroism instrumentation [62] our results underline again the need of control experiments when analyzing processes involving proteins, if protein structures are particularly sensitive to oxidation. Indeed, measurements themselves may cause structural modifications in proteins, probably even under slightly destabilizing conditions, and more easily in the absence of tryptophanil residues in the protein chain. The results here reported are relevant as they give a warning for pharmaceutical applications and in particular reveal that UV-light exposure during biopharmaceuticals production and analysis steps may induce damages in proteins. Light exposure

may also occur during bulk storage of the proteins[46,63]. Presented results not only highlight the relevant role in these processes of tyrosine aromatic residues and of the environmental conditions, but also suggest a simple and low cost method to check and quantify possible damages via steady state and time resolved fluorescence measurements.

Importantly, FLIM data reveal the substantial overlap between the new autofluorescence peak and the signal referred in literature as "Amyloid intrinsic fluorescence". The signal here attributed to tyrosine oxidation exists in the same spectral range with analogous feature so that it may represent a significant hindrance in the specific detection of amyloid intrinsic fluorescence. It is also possible to infer that the electronic levels that become available when tyrosine is oxidized both in vivo and in vitro may be at least one component of the dim blue signal which make fibrils observable in the visible range with standard laser scanning confocal or two photon microscopes.

Methods

Sample preparation

Ubiquitin from bovine erythrocytes, recombinant Human Insulin and Thioflavin T were purchased from Sigma Aldrich and used without further purification. Aβ(1–40) was purchased from Biopeptide and pre-treated as previously reported[64].

All experiments on UBQ samples were performed in 20 mM sodium phosphate buffer, pH 6.5. The sample was freshly prepared and filtered through 0.20 µm filters (17761, Sartorious), just before the measurements. Different protein concentrations had been used: 0.5 mg/ml, 0.7 mg/ml and 1.8 mg/ml. Protein concentration was spectrophotometrically determined using a molar extinction coefficient of 1254 $dm^3mol^{-1}cm^{-1}$ at 280 nm[31]. Human Insulin powder (Sigma-Aldrich) and Aβ(1-40) peptide (prepared as described in[65]), were dissolved in 20mM sodium phosphate buffer, pH 6.5.

Protein concentration of Human insulin and Aβ(1-40) peptide were estimated by means of absorbance measurements using a molar extinction of 1.067 cm^{-1} $(mg/ml)^{-1}$ at 276 nm[66], and of 1390 M^{-1} cm^{-1} at 276nm, respectively[67].

In order to obtain aggregates, 0.2 mg/ml Human insulin in 20 mM sodium phosphate buffer, pH 6.5, was incubated at 60°C stirring at500 rpm for 24 hours, and 0.2 µM Aβ(1–40) in 20 mM sodium phosphate buffer, pH 6.5, was incubated at 37 degrees with stirring 500 rpm for 24 hours. Resulting aggregates were found to be positive to Thioflavin T test.

UV-absorption:

Absorption measurements were carried out on a Jasco V-760 Spectrophotometer. Before and after each experiment samples were placed in 1 cm path quartz cuvette and absorption spectra were recorded. Absorption spectra were acquired from 200 to 600 nm, using a scan speed of 100 nm/ min, 1 nm bandwidth, data intervals of 0.5 nm and response of 0.96 s.

Circular Dichroism measurements

Circular dichroism (CD) measurements in the Far-UV region were performed using a Jasco J-715 spectropolarimeter equipped with a Jasco PCT 348WI temperature controller. Spectra were recorded from 270 to 190 nm, before and after treatment, using a scan speed of 50 nm/min, a 1 nm bandwidth and a data pitch of 0.1 nm. Each spectrum is the result of the average of 5 accumulations.

Fluorescence and Rayleigh scattering:

Fluorescence and Rayleigh scattering measurements were carried out on Jasco FP-8500 spectrofluorimeter equipped with a Jasco ETC-815 peltier as temperature controller.

Kinetic measurements:

Modifications in protein structures and aggregation kinetics were analyzed by in situ kinetic measurements.

All samples were placed in a 1 cm path quartz cuvette and spectra were recorded at 0.5 nm wavelength intervals, with excitation and emission bandwidth of 5 nm, scan-speed of 100 nm/min and integration time of 1 s. Intrinsic fluorescence emission spectra were acquired in the range 270–700 nm with excitation at 275 nm. Simultaneously, Rayleigh scattering was also measured as the maximum of the elastic peaks of excitation light at 275 nm. Measurements are performed by opening the shutter at defined temporal interval. This allows to control e modify sample exposure to UV light. Measurements either on samples continuously exposed to irradiation or stored in the dark are also performed for comparison.

To compare the effects of different irradiation protocols, emission spectra of 0.5 mg/ml UBQ at 60 °C were obtained with excitation at 275 nm wavelength, under continuous irradiation, and under irradiation every 6 minutes or every 30 minutes, for the duration of spectrum acquisition.

UBQ sample aggregation was induced at 25°C by 500rpm stirring under continuous irradiation. For each sample, emission spectra at 25°C, before and after kinetics, were measured to monitor significant variations of the emission band profile.

3D Fluorescence spectra

In order to better characterize the features of steady state fluorescence spectrum of oxidized protein, measurements on 1.8 mg/ml UBQ after incubation at 60 degrees under continuous UV exposure were performed. 85 individual emission spectra (360-700 nm) at sequential 2 nm increments of excitation wavelength between 280 and 450 nm, were acquired, using the

bandwidths for excitation and emission of 5 nm, scan-speed of 100 nm/min and integration time of 1 s.

Fluorescence Lifetime Imaging Microscopy (FLIM)

FLIM data of UBQ, Human Insulin and A-β(1-40) peptide were acquired in the time domain by means a Leica TCS SP5 inverted microscope with a 63× oil objective (Leica Microsystems) equipped with picoHarp 300 standalone TCSPC module (Picoquant). Thus 256 × 256 images were acquired at a scanning frequency of 200 Hz under two-photon excitation at 780 nm (Spectra-Physics Mai-Tai Ti:Sa ultra-fast laser).

FLIM data were processed by the SimFCS software developed at the Laboratory of Fluorescence Dynamics, University of California at Irvine. FLIM calibration of the system is performed by measuring the known lifetime of the fluorescein that is a single exponential of 4.0 ns. Every pixel of the FLIM image is transformed to a point in the phasor plot, the coordinates *g* and *s* (sine and cosine transforms, respectively) of each point in the phasor plot were calculated from the fluorescence-intensity decay in the corresponding pixel in the FLIM image as described by *Digman* et al*., 2008*[49] Details of the analysis are reported elsewhere[49,50,68]. Briefly: every possible lifetime is mapped in a phasor plot. All possible single exponential lifetimes lie on the "universal circle," defined as the semicircle going from point (0, 0) to point (1, 0), with radius 1/2. Point (1, 0) corresponds to $\tau = 0$, and point (0, 0) to $\tau = \infty$. Longer lifetimes are mapped near the origin and shorter lifetimes are mapped on the circumference toward the bottom right intersection with the x axis. In the phasor coordinates the single lifetime components add directly because the phasor follows the vector algebra. The clouds of points representing the fluorescence lifetime distribution over the two images are selected using a colored cursor the corresponding pixels are mapped back with selected color to the image pixels. [49,50,68]

Acknowledgements

We wish to thank Prof. Annalisa Pastore and Prof. Maurizio Leone for useful discussions a. Fluorescence microscopy measurements were acquired at “Microscopy and Bio-imaging Lab”, Mediterranean Center for Human Health Advanced Biotechnologies (CHAB), Aten Center, University of Palermo.

References:

1. Santos, A. L. & Lindner, A. B. Protein Posttranslational Modifications: Roles in Aging and Age-Related Disease. *Oxidative Medicine and Cellular Longevity.* **19** (2017).
2. Stadtman, E. R. Protein oxidation and aging. *Free Radic. Res.* **40,** 1250–1258 (2006).
3. Uttara, B., Singh, A. V, Zamboni, P. & Mahajan, R. T. Oxidative stress and neurodegenerative diseases: a review of upstream and downstream antioxidant therapeutic options. *Curr. Neuropharmacol*. **7,** 65–74 (2009).
4. Dalle Donne, I., Rossi, R., Colombo, R., Giustarini, D. & Milzani, A. Biomarkers of oxidative damage in human disease. *Clin. Chem*. **52,** 601–623 (2006).
5. Cai, Z. & Yan, L.-J. Protein Oxidative Modifications: Beneficial Roles in Disease and Health. *J Biochem Pharmacol Res.* **1**(1), 15–26 (2013).
6. Wall, S. B., Oh, J. Y., Diers, A. R. & Landar, A. Oxidative modification of proteins: An emerging mechanism of cell signaling. *Front. Physiol*. **3,** 1–9 (2012).
7. Davies, K. J. & Delsignore, M. E. Protein damage and degradation by oxygen radicals. III. Modification of secondary and tertiary structure. *J. Biol. Chem*. **262**, 9908–9913 (1987).
8. Birben, E., Sahiner U.M., Sackesen C., Erzurum S. and Kalayci O. Oxidative Stress and Antioxidant Defense. *World Allergy Organization Journal* **5,** 9–19 (2012).
9. Berlett, B. S. Protein oxidation in aging, disease, and oxidative stress. *J Biol Chem* **272**, 20313–20316 (1997).
10. Karran, P. & Brem, R. Protein oxidation, UVA and human DNA repair. DNA Repair (Amst). **44,** 178–185 (2016).
11. Murphy, M. P. How mitochondria produce reactive oxygen species. *Biochem. J.* **417**, 1–13 (2009).

12. Neves-Petersen, M. T. Klitgaard S., Pascher T., Skovsen E., Polivka T., Yartsev A., Sundström V., and Petersen S.B. Flash photolysis of cutinase: Identification and decay kinetics of transient intermediates formed upon UV excitation of aromatic residues. *Biophys. J.* **97,** 211–226 (2009).

13. Stadtman, E. R. & Levine, R. L. Free radical-mediated oxidation of free amino acids and amino acid residues in proteins. *Amino Acids* **25,** 207–218 (2003).

14. Giulivi, C., Traaseth, N. J. & Davies, K. J. A. Tyrosine oxidation products: Analysis and biological relevance. *Amino Acids* **25,** 227–232 (2003).

15. Heinecke, J. W. Tyrosyl radical production by myeloperoxidase: A phagocyte pathway for lipid peroxidation and dityrosine cross-linking of proteins. *Toxicology* **177**, 11–22 (2002).

16. Malencik, D. A. & Anderson, S. R. Dityrosine as a product of oxidative stress and fluorescent probe. *Amino Acids* **25,** 233–247 (2003).

17. Lehrer, S. S. & Fasman, G. D. Ultraviolet Irradiation Effects in Poly-L-tyrosine and Model Compounds. Identification of Bityrosine as a Photoproduct. *Biochemistry* **6,** 757–767 (1967).

18. Menter, J. M., Abukhalaf, I. K., Patta, A. M., Silvestrov, N. A. & Willis, I. Fluorescence of putative chromophores in Skh-1 and citrate-soluble calf skin collagens. *Photodermatol. Photoimmunol. Photomed.* **23,** 222–228 (2007).

19. Smith, G. J. & Haskell, T. G. The fluorescent oxidation products of dihydroxyphenylalanine and its esters. *J. Photochem. Photobiol. B Biol.* **55,** 103–108 (2000).

20. Al-Hilaly, Y. K., Biasetti, L., Blakeman, B. J. F., Pollack,S. J., Zibaee,S., Abdul-Sada,A., Thorpe,J. R., Xue, W. & Serpell, L.C. The involvement of dityrosine crosslinking in α-synuclein assembly and deposition in Lewy Bodies in Parkinson's disease. *Sci. Rep***. 6,** 1–13 (2016).

21. Correia, M., Neves-Petersen, M. T., Jeppesen, P. B., Gregersen, S. & Petersen, S. B. UV-Light Exposure of Insulin: Pharmaceutical Implications upon Covalent Insulin Dityrosine Dimerization and Disulphide Bond Photolysis. *PLoS One* **7,** (2012).

22. Wördehoff, M. M., Shaykhalishahi, H., Groß, L., Gremer, L., Stoldt, M., Buell, A.K., Willbold, D., Hoyer, W. Opposed Effects of Dityrosine Formation in Soluble and Aggregated α-Synuclein on Fibril Growth. *J. Mol. Biol*. **429,** 3018–3030 (2017).

23. Senadhi Vijay-Kumar, Charles E. Bugg, 3 and & Cook', W. J. Structure of Ubiquitin Refined at 1.8 A Resolution. .*I. Mol. Bid*. **194**, 531–544 (1987).

24. Ibarra-Molero, B., Loladze, V. V., Makhatadze, G. I. & Sanchez-Ruiz, J. M. Thermal versus guanidine-induced unfolding of ubiquitin. An analysis in terms of the contributions from charge-charge interactions to protein stability. *Biochemistry* **38,** 8138–8149 (1999).

25. Lindorff-Larsen, K., Best, R. B., Depristo, M. A., Dobson, C. M. & Vendruscolo, M. Simultaneous determination of protein structure and dynamics. *Nature* **433,** 128–132 (2005).

26. Walsh, C. T., Garneau-Tsodikova, S. & Gatto, G. J. Protein posttranslational modifications: The chemistry of proteome diversifications. *Angew. Chemie - Int. Ed.* **44,** 7342–7372 (2005).

27. Spasser, L. & Brik, A. Chemistry and biology of the ubiquitin signal. *Angew. Chemie - Int. Ed*. **51**, 6840–6862 (2012).

28. Yi, D. & Perkins, P. D. Identification of Ubiquitin nitration and oxidation using a liquid chromatography/mass selective detector system. *J. Biomol. Tech*. **16,** 362–368 (2005).

29. Choi, J., Martin, W. E., Murphy, R. C. & Voelker, D. R. Phosphatidylcholine and N -Methylated Phospholipids Are Nonessential in Saccharomyces cerevisiae. **279,** 42321–42330 (2004).

30. Chan, F. T. S., Kaminski Schierle, GS., Kumita,JR., Bertoncini,CW., Dobson, CM., and Kaminskia,CF. Protein amyloids develop an intrinsic fluorescence signature during aggregation. *Analyst* **138,** 2156–2162 (2013).

31. Noronha, M., Lima, J. C., Bastos, M., Santos, H. & Maçanita, A. L. Unfolding of ubiquitin studied by picosecond time-resolved fluorescence of the tyrosine residue. *Biophys. J.* **87,** 2609–2620 (2004).

32. Antosiewicz, J. M. & Shugar, D. UV–Vis spectroscopy of tyrosine side-groups in studies of protein structure. Part 2: selected applications. *Biophys. Rev.* **8,** 163–177 (2016).

33. Dancewicz, G. B. and A. M. Radiation-induced dimerization of tyrosine and glycyltyrosine in aqueous solutions. *INT. J . RADIAT. BIOL .*, **39,** 163–174 (1981).

34. Pickart, C. M., Haldeman, M. T., Kasperek, E. M. & Chen, Z. Iodination of tyrosine 59 of ubiquitin selectively blocks ubiquitin's acceptor activity in diubiquitin synthesis catalyzed by E225K. *J. Biol. Chem*. **267,** 14418–14423 (1992).

35. Munishkina, L. A. & Fink, A. L. Fluorescence as a method to reveal structures and membrane-interactions of amyloidogenic proteins. **1768,** 1862–1885 (2007).

36. Librizzi, F., Carrotta, R., Spigolon, D., Bulone, D. & San Biagio, P. L. α-Casein inhibits insulin amyloid formation by preventing the onset of secondary nucleation processes. *J. Phys. Chem. Lett.* **5,** 3043–3048 (2014).

37. Noronha, M., Gerbelová, H., Faria, TQ. , Lund, DN. , Smith, DA. , Santos, H. , Maçanita, AL. Thermal Unfolding Kinetics of Ubiquitin in the Microsecond-to-Second Time Range Probed by Tyr-59 Fluorescence. 9912–9919 (2010).

38. Giulivi, C. & Davies, K. J. A. Mechanism of the Formation and Proteolytic Release of H2O 2-induced Dityrosine and Tyrosine Oxidation Products in Hemoglobin and Red Blood Cells. *J. Biol. Chem.* **276,** 24129–24136 (2001).

39. Rayner, D. M., Krajcarski, D. T. & Szabo, A. G. Excited state acid–base equilibrium of tyrosine. *Can. J.Chem.* **56,** 1238–1245 (1978).

40. Heineckes, J. W., Li, W., Daehnke, H. L. & Goldstein, J. A. Dityrosine, a Specific Marker of Oxidation,.**202**, (1993).

41. Correia, M., Snabe, T., Thiagarajan,V., Petersen,S.B., Campos, SRR., Baptista,A.B., Neves-Petersen MR. Photonic activation of plasminogen induced by low dose UVB. *PLoS One* **10**, (2015).

42. Vetri V, Foderà V., The route to protein aggregate superstructures: Particulates and amyloid-like spherulites. *FEBS Lett.* **589,**(19 Pt A):2448-63(2015)

43. Reeg, S. & Grune, T. Protein Oxidation in Aging : Does It Play a Role in Aging Progression ? **23,** 239–255 (2015).

44. Groenning, M. Binding mode of Thioflavin T and other molecular probes in the context of amyloid fibrils-current status. *J. Chem. Biol*. **3,** 1–18 (2010).

45. Vine, H. Le. Quantification of beta-Sheet Amyloid Fibril Structures with Thioflavin T. *Methods Enzymol.* **309,** 274–284 (1999).

46. Foderà, V., Librizzi, F., Groenning, M., Van De Weert, M. & Leone, M. Secondary nucleation and accessible surface in insulin amyloid fibril formation. *J. Phys. Chem. B* **112,** 3853–3858 (2008).

47. Foderà, V., Groenning, M., Vetri,V., Librizzi,F., Spagnolo,S., Cornett,C., Lars Olsen, L., Marco van de Weert, M., and Leone, M. Thioflavin T hydroxylation at basic pH and its effect on amyloid fibril detection. *J. Phys. Chem. B* **112,** 15174–15181 (2008).

48. Chan, F. T. S., Kaminski, G. S., Kumita, J. R. & Bertoncini, C. W. Europe PMC Funders Group Protein amyloids develop an intrinsic fluorescence signature during aggregation. **138,** 2156–2162 (2017).

49. Digman, M. A., Caiolfa, V. R., Zamai, M. & Gratton, E. The phasor approach to fluorescence lifetime imaging analysis. *Biophys. J.* **94,** 14–16 (2008).

50. Lakner, P. H., Monaghan, M. G., Möller, Y. & Olayioye, M. A. Applying phasor approach analysis of multiphoton FLIM measurements to probe the metabolic activity of three- dimensional in vitro cell culture models. *Nat. Publ. Gr.* **1**–11 (2017)

51. Cai, Z., Zhao, B. &Ratka, A. Oxidative stress and β-amyloid protein in Alzheimer's disease. *NeuroMolecular Medicine* **13,** 223–250 (2011).

52. Park, K., Gross, M., Lee, D.-H., Holvoet, P., Himes, J.H., Shikany, J.M., Jacobs Jr., D. R. Oxidative Stress and Insulin Resistance The Coronary Artery Risk Development in Young Adults study. 3–8 (2009).

53. Vilasi, S., Picone, P., Vilasi. S., Librizzi, F., Contardi, M., Nuzzo,D.,Caruana,L., Baldassano,S., Amato,A., Mulè,F., San Biagio,PL., Giacomazza,D., and Di Carlo, M. Biological and biophysics

aspects of metformin - induced effects : cortex mitochondrial dysfunction and promotion of toxic amyloid pre - fibrillar aggregates. **8**, 1718–1734(2016).

54. Picone P., Nuzzo D., Caruana L., Messina E., Barera A., Vasto S., Di Carlo M. Metformin increases APP expression and processing via oxidative stress, mitochondrial dysfunction and NF- κ B activation : Use of insulin to attenuatemetformin ' s effect. *Biochimica et Biophysica Acta - Mol. Cell Res*. **1853,** 1046–1059 (2015).

55. Asanuma, M., Miyazaki, I. & Ogawa, N. Dopamine- or L-DOPA-induced neurotoxicity: The role of dopamine quinone formation and tyrosinase in a model of Parkinson's disease. *Neurotox. Res.* **5,** 165–176 (2003).

56. Mach, H., Middaugh, C. R. & Lewis, R. V. Statistical determination of the average values of the extinction coefficients of tryptophan and tyrosine in native proteins. *Anal. Biochem*. **200,** 74–80 (1992).

57. Ghisaidoobe, A. B. T. & Chung, S. J. Intrinsic tryptophan fluorescence in the detection and analysis of proteins: A focus on Förster resonance energy transfer techniques. *Int. J. Mol. Sci*. **15,** 22518–22538 (2014).

58. Van Maarschalkerweerd A, Pedersen MN, Peterson H, Nilsson M, Nguyen TTT, Skamris T, Rand K, Vetri V, Langkilde AE, and Vestergaard B, Formation of covalent di-tyrosine dimers in recombinant α-synuclein. *Intrinsically Disord. Proteins* **3**, (2015).

59. Al-Hilaly Y. K., Williams T. L., Stewart-Parker M., Ford L., Skaria E., Cole M., Bucher W. G., Morris K. L., Abdul Sad A., Thorpe J. R. and Serpell L. C. A central role for dityrosine crosslinking of Amyloid-β in Alzheimer's disease. *Acta Neuropathologica Communications* **1,** (2013).

60. Thal DR., Ghebremedhin E, Haass C, Schultz C. UV light-induced autofluorescence of full-length Abeta-protein deposits in the human brain. *Clin. Neuropathol*. **1**,35-40(2002).

61. Tikhonova, T. N., Rovnyagina NR, Zherebker AY, Sluchanko NN, Rubekina AA, Orekhov AS, Nikolaev EN, Fadeev VV, Uversky VN, Shirshin EA. Dissection of the deep-blue autofluorescence changes accompanying amyloid fibrillation. *Arch. Biochem. Biophys***. 651,** 13–20 (2018).

62. Balasubramanian, D., Guptasarma, P., Luthra, MannIn Situ Photoreactions of Proteins in Spectrometers Leading to Variations in Signal Intensities. *Journal of the American Chemical Society.* **5,** 1877-1878 (1992).

63. Nitin Rathore, and R. S. RajanCurrent Perspectives on Stability of Protein Drug Products during Formulation, Fill and Finish Operations. *Biotechnol. Prog*. **24,** 504–514 (2008).

64. Hayrabedyan, S., Todorova, K., Spinelli, M., Barnea, E. R. & Mueller, M. The core sequence of PIF competes for insulin/amyloid β in insulin degrading enzyme-potential treatment for Alzheimer`s disease. **9,** 33884–33895 (2018).

65. D'Amico, M., Di Carlo, M.G., Groenning, M., Militello, V., Vetri, V., and Leone, M. Thioflavin T promotes Aβ(1-40) amyloid fibrils formation. *J. Phys. Chem. Lett***. 3,**1596–1601 (2012).

66. Manno, M., Craparo, E. F., Martorana, V., Bulone, D. & San Biagio, P. L. Kinetics of insulin aggregation: Disentanglement of amyloid fibrillation from large-size cluster formation. *Biophys. J.* **90,** 4585–4591 (2006).

67. Di Carlo, M. G., Minicozzi, V., Foderà, V., Militello, V., Vetri, V., Morante, S., Leone, M. Thioflavin T templates amyloid β(1-40) conformation and aggregation pathway. *Biophys. Chem.* **206,** 1–11 (2015).

68. Stringari,C., Cinquin,A., Cinquin,O., Digman, M.A., Donovan,P.J., & Gratton E. Phasor approach to fluorescence lifetime microscopy distinguishes different metabolic states of germ cells in a live tissue. *Proc. Nat. Ac. Sci.* **108** 13582-13587 (2011)